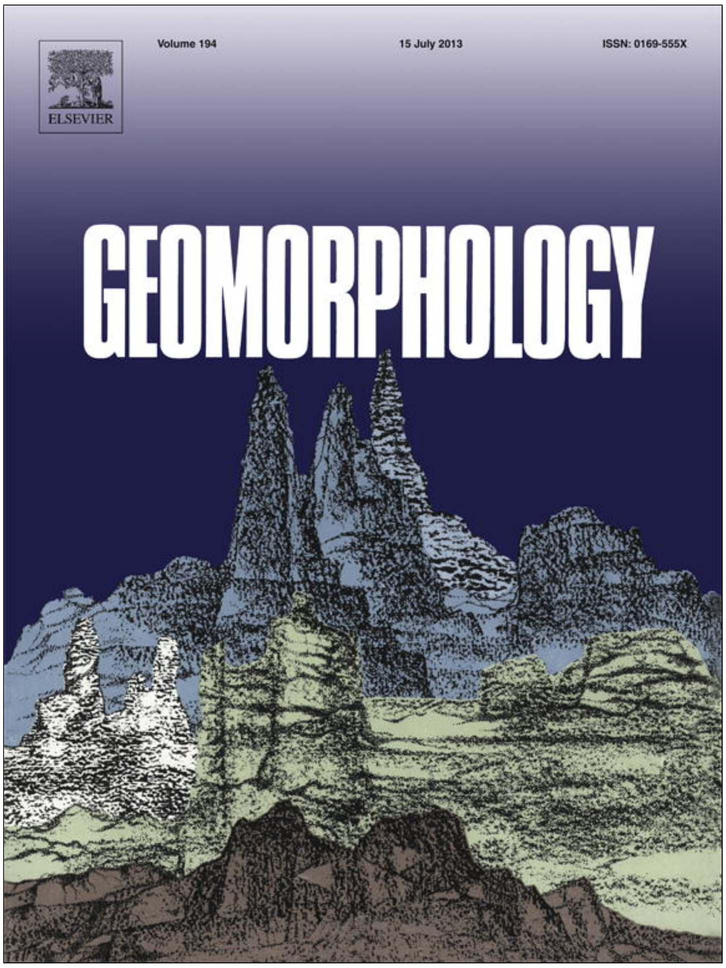
Volume 194
15 July 2013
ISSN: 0169-555X
ELSEVIER
GEOMORPHOLOGY

Geomorphology 194 (2013) 108–120

Contents lists available at SciVerse ScienceDirect

Geomorphology

journal homepage: www.elsevier.com/locate/geomorph

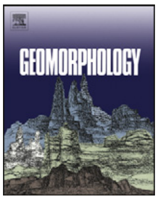

Recent decadal growth of the Atchafalaya River Delta complex: Effects of variable riverine sediment input and vegetation succession

Timothy Rosen, Y. Jun Xu *

School of Renewable Natural Resources, Louisiana State University Agricultural Center, Baton Rouge, LA 70803, USA

ARTICLE INFO

Article history:
Received 11 August 2012
Received in revised form 5 April 2013
Accepted 8 April 2013
Available online 20 April 2013

Keywords:
Delta progradation
Sediment yield
Vegetative stabilization
Atchafalaya River
Mississippi River Delta

ABSTRACT

The Mississippi River Delta Plain has experienced substantial wetland loss from subsidence, erosion, and sea level rise, threatening coastal communities and the ecosystems that support them. The Atchafalaya River, the largest distributary of the Mississippi River, has one of the few prograding delta features along the ~200-km deltaic coastline. Understanding changes in the Atchafalaya River Delta complex (ARDC) development has critical implications for future prediction and management strategy for the Mississippi River Delta Plain. This study was organized to answer two major questions: (1) how did development of the ARDC respond to fluctuation in riverine sediment supply over the period 1989–2010, and (2) has vegetation succession helped stabilize subaerial land? The study quantified annual total suspended sediment yields to the two ARDC subdeltas—Atchafalaya River subdelta (ARSD) and Wax Lake outlet subdelta (WLSD)—classified delta land cover using satellite imagery over ~5-year intervals into three classes: barren land, vegetation, and open water and investigated the relationship of delta land change with sediment yield and vegetation succession. Over the entire 21-year study period, we found a net land gain of 59 km^2, with the ARSD accounting for 58% of this gain and WLSD 42%. Sediment yield to the subdeltas decreased from an average annual of 38 megatonnes (MT) for ARSD and 18 MT for WLSD during 1989–1995 to an average annual of 24 MT for ARSD and 17 MT for WLSD during 2004–2010, corresponding to the decrease in riverine suspended sediment concentration. Concurrently, total land growth rate decreased from 2.4 $km^2\ y^{-1}$ to 1.6 $km^2\ y^{-1}$ for ARSD and 3.2 $km^2\ y^{-1}$ to 0.6 $km^2\ y^{-1}$ for WLSD. However, the ARDC had a net land loss of 2.1 km^2 during 1999–2004 because of tropical system effects in conjunction with the lack of large river floods (defined as discharge > 13,800 $m^3\ s^{-1}$). On average, more than 60% of newly vegetated land remained vegetated in subsequent years, and when compared with barren areas, vegetated land was less likely (7.3% vs. 32%) to be converted to water, indicating vegetative stabilization effect. However, during the period without a major flood, vegetation buffering against tropical system erosion was limited. This indicates that over the period 1989 to 2010 land growth of the ARDC was dictated by large flood events.

1. Introduction

Among coastal margins, deltas may be the most economically important regions, serving as transportation hubs and commercial centers while providing abundant natural resources that support large populations of people and wildlife. However, many of the world's deltas today are under unprecedented pressure from land loss because of reduced riverine sediment supply (e.g., Walling and Fang, 2003), coastal land erosion (e.g., Smith and Abdel-Kader, 1988; Chen and Zong, 1998), subsidence (e.g., Day et al., 1995; Syvitski et al., 2009), and sea level rise (e.g., Day et al., 1995; Gornitz, 1995). As with other delta regions, the Mississippi River Delta Plain has not been immune from land loss and has had one of the most significant conversions of land to open water, with over 4877 km^2 submerged since 1932, endangering large coastal communities (Couvillion et al., 2011). This loss has been attributed to rapid subsidence of Holocene strata (Törnqvist et al., 1996, 2008), exacerbated by the reduction in riverine sediment supply (Kesel, 2003), hydrocarbon extraction (Morton and Bernier, 2010), local faults, and glacial isostatic adjustment (Yuill et al., 2009). With much of the delta plain under stress, research and management interests have been building in the Atchafalaya River Delta complex (ARDC), the only noticeable prograding delta feature along the Mississippi River Delta coastline.

The Mississippi River enters the Gulf of Mexico through two distributaries: the Mississippi River main channel southeast of New Orleans, Louisiana, and the Atchafalaya River located to the west on the Louisiana central coast. The Atchafalaya River is ~190 km long, flowing southward through a levee-confined floodplain area of 4921 km^2, much of which is riparian forested swamps (Ford and Nyman, 2011). Since the early twentieth century, because of human alterations to the Atchafalaya River and a more favorable gradient than the Mississippi River, a well-defined channel began to form, which increased the flow volume going down the

---

* Corresponding author. Tel.: +1 225 578 4168; fax: +1 225 578 4227.
E-mail address: yjxu@lsu.edu (Y.J. Xu).

0169-555X/$ – see front matter © 2013 Elsevier B.V. All rights reserved.
http://dx.doi.org/10.1016/j.geomorph.2013.04.020

Atchafalaya River (Fisk, 1952; Roberts et al., 1980). The increased discharge caused many of the open water areas in the Atchafalaya River basin to accumulate sediments, losing much of the open water and swamp habitat to lacustrine delta formations (Tye and Coleman, 1989). With the open water areas sediment filled, formation of subaqueous deltas at the two outlets of the Atchafalaya River, Morgan City main channel (ARMC) and Wax Lake outlet (WLO), became noticeable in the 1950s (Shlemon, 1975). Subaerial land started forming in 1972 and was accelerated by large floods that occurred from 1973 to 1975, forming the Atchafalaya River subdelta (ARSD) and Wax Lake Outlet subdelta (WLSD) (Roberts et al., 1980). With subaerial delta formation, vegetation succession was able to begin with emergent plants colonizing once the delta islands reached intertidal elevations. By 1979, the Atchafalaya River Delta had over 16 km^2 vegetated (Johnson et al., 1985).

Several factors may have affected deltaic growth of the ARDC: sediment load, tropical systems, cold fronts, and vegetation colonization. Rouse et al. (1978) observed high growth rate of the ARSD following the 1973, 1974, and 1975 river floods. Barras (2007) found that hurricane Rita in 2005 removed much of the submerged aquatic vegetation and floating vegetation in the ARDC, while also enlarging existing ponds. Hurricane Andrew in 1992 was documented adding, on average, 16 cm of accumulated sediment to marshes surrounding the Atchafalaya Bay (Guntenspergen et al., 1995), while Walker (2001) found that hurricanes can also cause sediment-laden water to be transported off the coast, away from the ARDC. Cold frontal passage has also been documented transporting sediment out of Atchafalaya Bay, with an estimate of 400,000 t per front, which equates to ~10.6 megatonnes (MT) during a year (Walker and Hammack, 2000; Roberts et al., 2005). This erosion reduces the rate of subaerial delta development and leaves the delta features sandy (van Heerden and Roberts, 1980). Johnson et al. (1985) noted that with the colonization of plant species (most notably *Salix nigra*) physical processes were aided by biotic controls to enhance sedimentation and stabilization of the ARDC, although the long-term effect of vegetation on delta land growth in the ARDC is unclear. The above studies identify separate factors that have affected delta growth, but no systematic longer-term look into how the ARDC subdeltas have responded to varying sediment input and environmental stressors has been undertaken.

With the decline of total suspended sediment throughout the Mississippi River (Horowitz, 2010; Heimann et al., 2011) it has become imperative to track changes in total suspended sediment discharge to coastal Louisiana and the impacts on coastal processes. Sediment supply is one the most important components that shape delta growth (Orton and Reading, 1993). However, uncertainty exists regarding how much sediment is discharged from ARMC and WLO to the subdeltas. Previous studies have documented sediment discharge to the ARDC from sediment data collected from the upper Atchafalaya River (Rouse et al., 1978), but Xu (2010) reported that there is a 9% sediment load reduction in the Atchafalaya River basin before reaching the outlets, fluctuating with the river hydrological conditions. With new management plans that have suggested diversions from the Atchafalaya River to other coastal areas in Louisiana (CPRA, 2012), there is an urgent need to have a comprehensive assessment on riverine sediment discharge and how the quantity and fluctuation of the sediment discharge and vegetation succession may have influenced land growth in the ARDC. This assessment is critical since different delta progradation at the two river outlets have been reported (e.g., Barras, 2007; Xu, 2010; Couvillion et al., 2011).

Using this background information, we conducted this study to take a longer-term (1989–2010) look at total suspended sediment discharge to the Atchafalaya River subdeltas below Morgan City and Wax Lake outlet to assess how this may have affected delta land change over four ~5-year periods (i.e., 1989 to 1995, 1995 to 1999, 1999 to 2004, and 2004 to 2010). The primary purposes of the study were to determine the relation of ARDC development to total suspended sediment discharge from the river's two outlets and to assess the role that vegetation succession may have played in stabilizing newly created land. The results are discussed in light of the influencing factors introduced earlier.

2. The Atchafalaya River Delta complex

The Atchafalaya River Delta complex is composed of two subdeltas, Atchafalaya River subdelta (ARSD) and Wax Lake outlet subdelta (WLSD), extending approximately from 29°23′ N. to 29°32′ N. in latitude and from 91°15′ W. to 91°30′ W. in longitude (Fig. 1). Both of these features are building into the shallow, low energy (mean wave height ~ 0.5 m), microtidal (mean tidal range 0.35 m) Atchafalaya Bay and display typical lobate delta growth of a river-dominated delta, based on Galloway's delta classification (1975). Current subaqueous delta clays extend out to the 8-m isobath outside of the Atchafalaya Bay (Neill and Allison, 2005). The ARDC is fed by the Atchafalaya River that carries a portion of the Mississippi River's flow and the entire flow from the Red River. The flow portion from the Mississippi River is controlled by a diversion structure, the Old River Control Structure (ORCS) that was built in 1963 to prevent the avulsion of the Mississippi River into the channel of the Atchafalaya River. Under normal flow conditions, the ORCS maintains 24 ± 3% (Horowitz, 2010) of the Mississippi River discharge but ~30% to 60% of the Mississippi River's total suspended sediment yield (Mossa and Roberts, 1990; Horowitz, 2010). In recent years, on average, the Mississippi River's water contributes about two-thirds of the entire Atchafalaya's discharge, but the Red River could make up to 70% of the river discharge during the low flow period of the Mississippi River (Xu and BryantMason, 2011). The ARDC is located in humid subtropical climate (Köppen climate classification *Cfa*) and is affected by tropical systems (hurricanes and tropical storms) and strong cold fronts. Vegetation of the ARDC varies by elevation and successional stage, but commonly found genera are *Sagittaria*, *Salix*, *Typha*, *Polygonum*, *Nelumbo*, and *Phragmites*.

3. Methods

3.1. Discharge, total suspended sediment, and tropical systems

Daily mean discharge data were downloaded from the U.S. Geological Survey (USGS) website (http://waterdata.usgs.gov/la) for lower Atchafalaya River at Morgan City, Louisiana (ARMC, 29°41′33.4″ N., 91°12′42.6″ W.; Fig. 1), and Wax Lake outlet at Calumet, Louisiana (WLO, 29°41′52″ N., 91°22′22″ W.; Fig. 1). Discharge measurement did not begin at ARMC until October 1995. Missing discharge data for ARMC were estimated back to 1989 based off of a relationship from Xu and Wang (in review) using data collected by the U.S. Army Corps of Engineers (USACE) at a gaging station upriver at Simmesport, Louisiana (ARS, 30°58′ 57″ N., 91°47′54″ W.). The relationship was ($r^2 = 0.89$):

$$\mathrm{QARMC} = 10894.31977 + 0.53129\,(\mathrm{QARS}) \tag{1}$$

where QARMC and QARS are the daily discharge passing ARMC and ARS ($m^3\ d^{-1}$). Annual maximum discharge data were also used from the Atchafalaya River Simmesport, Louisiana, to count the number of large flood events (discharge > 13,800 $m^3\ s^{-1}$, 34% flood exceedance). Suspended sediment concentration (SSC) data were downloaded from the USGS for ARMC and WLO. At ARMC and WLO, suspended sediment data are collected monthly during nonflood and bimonthly during flood seasons. During severe flood events, sediment data are collected more frequently by USACE and USGS. Suspended

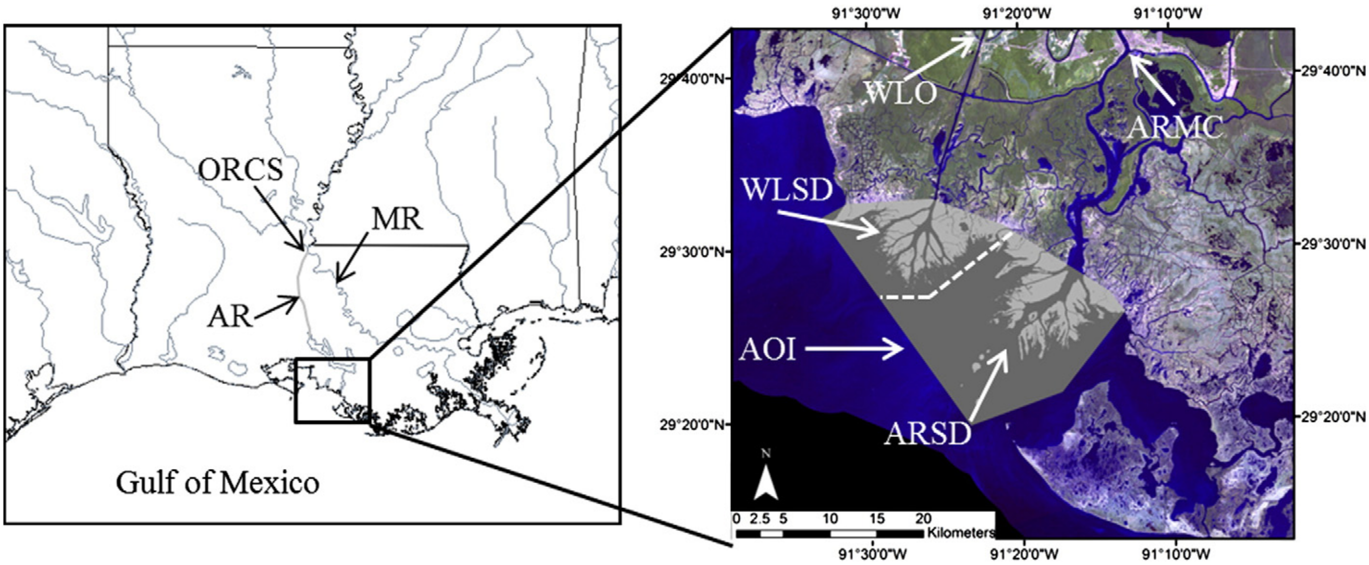

Fig. 1. Map of study area, AOI (area of interest) is the area subsetted for analysis. Light gray area is land and dark gray is water, and the dashed white line demarcates the subsetted areas for the Wax Lake outlet subdelta (WLSD) and the Atchafalaya River Morgan City subdelta (ARSD). The ARMC is Atchafalaya River Morgan City station and WLO is Wax Lake outlet station, where discharge and suspended sediment concentration were collected. Old River control structure (ORCS) controls water flow from the Mississippi River (MR) to the Atchafalaya River (AR).

sediment data comprises both suspended sand and suspended mud and will be referred to as total suspended sediment.

Tropical systems that impacted the region were determined from Roth (2010). Hurricanes and tropical storms were counted to determine the total amount of tropical systems that impacted Louisiana for each period during the study (Table 1).

3.2. Total suspended sediment discharge calculation

Using SSC and daily discharge measured on the same dates, daily total suspended sediment load (SSL) was calculated as follows:

$$\text{Daily SSL}\left(\text{tonnes d}^{-1}\right) = \left[Q\left(\text{m}^3\text{s}^{-1}\right)\right]\left[\text{SSC}\left(\text{mg l}^{-1}\right)\right](0.00864). \tag{2}$$

Long-term daily total suspended sediment loads for ARMC and WLO were estimated using log–log linear regression and log–log second order polynomial regression equations relating measured daily total suspended sediment load to discharge:

$$\text{Linear regression: } \ln(\text{SSL}) = \ln(a) + b\ln(Q) + \varepsilon \tag{3}$$

$$\text{Second order polynomial regression: } \ln(\text{SSL}) = \ln(a) + b\ln(Q) - c\ln\left(Q^2\right) + \varepsilon \tag{4}$$

where SSL is daily total suspended sediment load; Q is discharge; *a*, *b*, and *c* are constants; and ε is lognormally distributed error (e.g., Miller, 1951; Glysson, 1987; Helsel and Hirsch, 2002). Both linear and second order polynomial sediment rating curves were calculated with and without smearing correction. Smearing correction was followed using the methods of Duan (1983). Long-term (using all the data) and three-year sediment rating curves were developed separately for each station using linear and second order polynomial regression. Three-year intervals were used because of no SSC values for 2006 at ARMC and WLO and only six SSC values available at WLO for the year 2007. The accuracy of the estimated values were evaluated by percentage difference between measured loads, calculated from Eq. (2), and estimated total suspended sediment load calculated from the sediment rating curves, based on Horowitz (2003):

$$\%\ \text{difference} = \{[(\text{predicted value}) - (\text{measured value})]/(\text{measured value})\} \times 100. \tag{5}$$

The rating curves with best-fitting parameters (see Appendix A) were selected to estimate total suspended sediment load (t d^{-1}) and subsequently summed in order to obtain total suspended sediment yield (t y^{-1}) on the annual scale from 1989 to 2010. Trend in long-term SSC, discharge, and total suspended sediment yield was determined by Seasonal Mann–Kendall test for trend using a DOS-based program developed by the USGS (Helsel et al., 2006).

3.3. Spatial data sets

For spatial land change analysis, cloud-free Landsat 5 images (Path 23, Row 40) for the years 1989, 1995, 1999, 2004, and 2010 (Table 2) were obtained from the USGS, Earth Resources Observation and Science Center. Dates of these images were also chosen based on river discharge (low discharge — September and October) and tide conditions to minimize water level effect on subaerial land assessment. Reported tide levels for the images were obtained from National Oceanic and Atmospheric Administration (NOAA) tide gage at Grand Isle, Louisiana (29°15′24″ N., 89°57′24″ W.; Table 2). Daily discharge data was used from ARMC (introduced earlier). River stage was not used because of its variability over time from changes in the river channel profile. Discharge was assumed to be consistent because it is recalibrated every several years to account for changes in stage. The study area was limited to both delta features and marsh areas that were proximal to the ARDC (Fig. 1).

3.4. Classification

Unsupervised classification was completed for each image using the ISODATA clustering method in ERDAS IMAGINE. The ARDC area was selected out from the original images based on the farthest extent of land and included some adjoining areas surrounding the deltas (Fig. 1). Twenty-five classes were derived in the classification

Table 1
Names and strengths of tropical systems that impacted Louisiana from 1989 to 2010.

Name	Year	Period	Category[a]	Distance[b] (km, direction)
Andrew	1992	1989–1995	3	20, W
Opal	1995	1989–1995	3	408, E
Josephine	1996	1995–1999	TS	184, E
Danny	1997	1995–1999	1	85 E
Frances	1998	1995–1999	TS	532, W
Georges	1998	1995–1999	2	286, E
Allison	2001	1999–2004	TS	Direct impact
Isidore	2002	1999–2004	TS	145, E
Lili	2002	1999–2004	1	63, W
Matthew	2004	2004–2010	TS	70, E
Katrina	2005	2004–2010	3	180, E
Rita	2005	2004–2010	3	236, W
Humberto	2007	2004–2010	1	246, W
Gustav	2008	2004–2010	2	70, E
Ike	2008	2004–2010	1	324, W

Category 3 = 178–208 km h^{-1}.

[a] Category is the Saffir–Simpson scale and identifies the wind strength of the storm at landfall. TS = Tropical storm, 63–118 km h^{-1}; category 1 = 119–153 km h^{-1}; category 2 = 154–177 km h^{-1}.

[b] Distance is the approximate distance the landfall was from ARDC.

with the maximum number of iterations set to 12 and the convergence threshold set to 0.99. The 25 classes were subsequently categorized in three basic cover types: (i) water, (ii) vegetation, and (iii) barren. These classes were derived based on true color Landsat imagery as well as plotting the classes over feature space images of Landsat bands 3 and 4. The vegetation cover type did not discriminate between vegetation on land or floating on water and from here on is discussed as vegetated land. After initial classification, mixed classes were identified using a cluster busting technique that used a mask to select the mixed class from the original image so that reclassification of the mixed class could be completed.

3.5. Land change analysis

Land change was determined by completing a matrix analysis in ERDAS IMAGINE using consecutive images. This was done for image pairs of 1989 vs. 1995, 1995 vs. 1999, 1999 vs. 2004, 2004 vs. 2010, and 1989 vs. 2010. A land change image was produced for each time frame with classes that fell into nine different categories: water no change, water to vegetation, water to barren, barren no change, barren to water, barren to vegetation, vegetation no change, vegetation to water, and vegetation to barren. Areas were calculated to determine changes over the different time frames. In all analyses, land gain is the addition of the areas for water to vegetation and water to barren; land loss is the addition of the areas for vegetation to water and barren to water. To complete separate area calculations for each subdelta, the land change images were subset to select out the ARSD and the WLSD (Fig. 1).

Table 2
Tide and discharge (Q) data for the time of Landsat image capture, and annual tide (MSL (min; max)), and annual Q (mean (min; max)) for the year the image was captured.

Date	Tide (m)	Q (m^3 s^{-1})	Annual tide (m)	Annual Q (m^3 s^{-1})
9/2/1989	0.11	2828	0.03 (−0.67; 0.52)	4004 (1436; 7616)
10/21/1995	0.19	3475	0.13 (−0.41; 0.71)	3614 (1541; 7916)
9/14/1999	0.21	2403	0.14 (−0.42; 0.64)	3509 (1135; 8022)
9/27/2004	0.37	4604	0.16 (−0.41; 1.03)	4043 (1752; 6804)
10/30/2010	0.13	2938	0.22 (−0.38; 0.83)	4006 (1586; 6939)

New land stability was determined in two steps: (i) selecting pixels that were converted from water to barren and water to vegetation, and (ii) assessing if the classified pixel value changed back to water in the subsequent image. To complete this, a matrix analysis was run using the matrix analysis land change images with the next consecutive classified image, for instance, the 1989 vs. 1995 matrix analysis was done with the 1999 classified image. This allowed for the identification of whether new subaerial land was maintained or lost. This was completed for both subdelta subsets and as an additional analysis for land that was lost.

4. Results

4.1. River discharge and total suspended sediment yield

Over the 21-year period, the Atchafalaya River had an average annual total flow volume of 200.0 km^3, varying between 122.7 km^3 (2000) and 252.8 km^3 (2009). About 118.7 km^3 of the average annual total flow volume (i.e., nearly 60%) passed through the ARMC outlet, with a low of 74.0 km^3 (2000) and a high of 164.1 km^3 (1993) (Fig. 2). The river's other outlet, WLO, had an average annual flow volume of 81.3 km^3, varying between 48.8 km^3 (2000) and 115.2 km^3 (2009) (Fig. 2). At the beginning of the study period (1989), ARMC discharged 65% and WLO 35% of the total flow volume, and the flow portions gradually changed to 53% for ARMC and 47% for WLO by 2010. The increasing trend of flow at WLO was significant ($p = 0.0504$, seasonal-Mann–Kendall). This increase was triggered by a weir removal in 1994 that had previously constricted flow down WLO. During the entire 21 years of this study a total of 10 major flood events occurred (when discharge was >13,800 m^3 s^{-1} at Atchafalaya River Simmesport, LA). Five of the flood events occurred during 1989–1995, two during 1995–1999, none from 1999 to 2004, and three during 2004–2010 (Table 3).

Average suspended sediment concentration was higher at ARMC (242 mg l^{-1}) than at WLO (227 mg l^{-1}) (Fig. 2). Annual average SSC at ARMC varied between 145 mg l^{-1} (2000) and 449 mg l^{-1} (1998), while annual average SSC at WLO varied between 136 mg l^{-1} (2000) and 351 mg l^{-1} (1998), with typically higher concentrations during high flow springs and lower concentrations during low flow summers and falls (data not shown). Over the study period, SSC decreased significantly at both ARMC ($p = 0.0235$, seasonal Mann–Kendall) and WLO ($p = 0.0337$, Seasonal Mann–Kendall). Over the entire 1989–2010 period, the Atchafalaya River discharged 1121.0 MT of total suspended sediment to the ARDC, averaging annually 51.0 MT with a range from 21.9 MT (2000) to 94.8 MT (1998). The ARMC discharged a total of 661.5 MT of total suspended sediment, averaging annually 31.8 MT and varying between 13.6 MT (2000) and 60.4 MT (1998) (Fig. 2). The WLO total suspended sediment discharge was 405.8 MT, averaging annually 19.2 MT, and ranging from 8.3 MT (2000) to 34.4 MT (1998) (Fig. 2). The ARMC accounted for 71% and the WLO 29% of the total suspended sediment discharged in 1989, while by 2010 ARMC accounted for 55% and WLO 45% of the sediment discharged. Over the 21-year period, the ARMC showed a significant decreasing trend in total suspended sediment yield ($p = 0.0276$, seasonal Mann–Kendall), while no clear trend was observed at the WLO. Between the four periods used in the spatial analysis, total suspended sediment yield decreased from an average annual high of 67 MT y^{-1} (1995–1999) to an average annual low of 41 MT y^{-1} (2004–2010) (Fig. 2).

4.2. Deltaic land change

From 1989 to 2010 the ARDC had a total new subaerial land gain of 62.0 km^2. The net subaerial land gain was 58.9 km^2 because of a

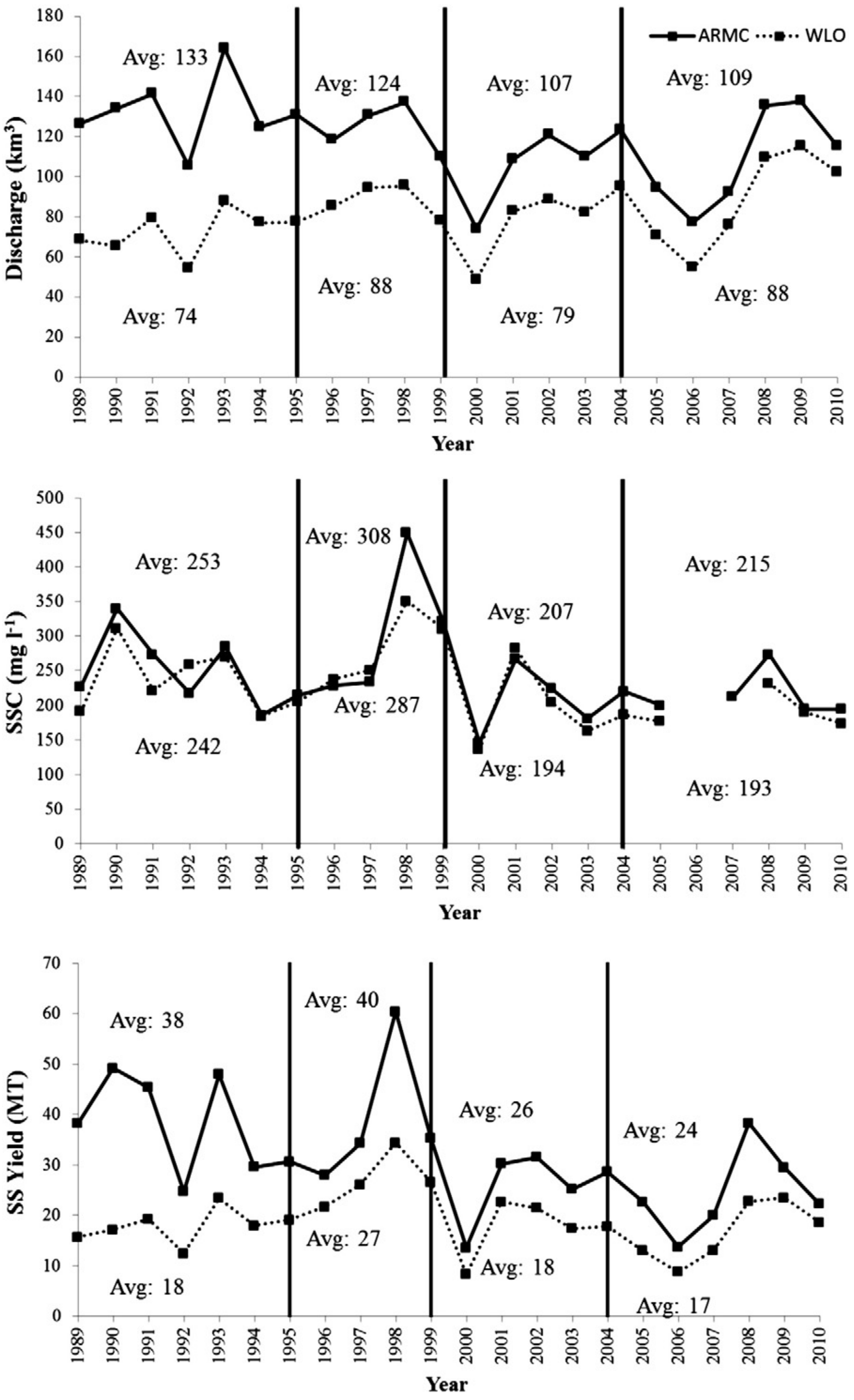

Fig. 2. Annual river flow volume (km^3), average annual SSC (mg l^{-1}), and annual total suspended sediment yield (MT), for Atchafalaya River Morgan City (ARMC) and Wax Lake outlet (WLO). Lines delineate between periods, values shown are mean annual values for each period.

loss of 3.1 km^2 (Table 4). The delta complex experienced a decrease in total land change rate from a high of 5.6 km^2 y^{-1} (1989–1995) to a low of -0.4 km^2 y^{-1} (1999–2004) (Table 4). The most recent period (2004–2010) saw a total land change rate of 2.1 km^2 y^{-1}. The period 1999 to 2004 had the largest amount of land lost, 16.6 km^2, and least amount of new land created, 14.5 km^2. The largest land gain, 37.3 km^2, and smallest amount lost, 3.7 km^2, occurred from 1989 to 1995. Over the entire 21-year period, annual land growth rate averaged 2.8 km^2 y^{-1}.

From 1989 to 2010 ARSD at the Morgan City river mouth had a net land gain of 34.4 km^2 (or 58% of the total new land in ARDC), while WLSD at the Wax Lake outlet river mouth had a net land gain of 24.6 km^2 (or 42% of the total new land in ARDC). Land growth at ARSD has been net positive throughout the study period, with the largest net gain of 14.6 km^2 during 1989–1995 (Fig. 3A) and the lowest net gain of 2.5 km^2 during 1999–2004 (Fig. 3B). The largest net land gain could have been partially influenced by the creation of dredge islands, especially apparent in the 1989–1995 period classified as barren land; while the net gain during 1989–1995 and 1995–1999 occurred more prominently as mouth bar island formation and elongation of channel levee areas. The 1999–2004 and 2004–2010 periods saw more land creation in distal areas. Land growth at WLSD was much more variable with a net loss of 4.6 km^2 of land from 1999 to 2004 and the largest net gain of 19.0 km^2 from 1989 to 1995. The net loss during 1999–2004 was predominantly located in distal areas of the delta away from the river mouth. Growth during the 1989–1995 and 1995–1999 periods consisted of total mouth bar island creation, whereas 2004–2010 growth mostly occurred near channel levee areas. The rate of land area growth for ARSD varied between 0.5 km^2 y^{-1} (1999–2004) (Fig. 3B) and 2.5 km^2 y^{-1} (1989–1995) (Fig. 3A), and for the entire period was 1.6 km^2 y^{-1}. Land change rates for WLSD fluctuated from a high of 3.2 km^2 y^{-1} (1989–1995, Fig. 3A) to a net loss of 0.9 km^2 y^{-1} (1999–2004; Fig. 3B); and the entire period had a net gain of 1.2 km^2 y^{-1}.

4.3. Vegetated land change

Of the 62 km^2 of new subaerial land gain since 1989, 87% of the land has been vegetated. For each period, land classified as vegetated land was converted less readily to open water than barren. The percent average of barren land converted to water was 32.0% between years, compared to only 7.3% of vegetated land. On average 57% of barren land was converted to vegetated land, whereas on average only 3.5% vegetated land was converted to barren land. The ARDC had a net vegetated land loss over the period 1999 to 2004, with 12.6 km^2 converted to open water (13% of the vegetated land in 1999). The largest net barren land loss also occurred over the same period, with 4.1 km^2 (39% of barren land in 1999) converted to open water. The largest net vegetated land gain occurred over the period 1989 to 1995, with 25.7 km^2 added to the deltas. The largest net barren land gain occurred over the same period with 7.9 km^2.

The ARSD accounted for 33.1 km^2 (61%) and WLSD accounted for 20.9 km^2 (39%) of the total newly vegetated land in the ARDC (1989–2010). The greatest net gain from open water to vegetated land in the WLSD was 16.6 km^2 over the period 1989 to 1995 (Fig. 3A). Net vegetated land gain was found at WLSD during all periods except for 1999 to 2004 (Fig. 3B). For the period 1989 to 1995, 87% of the net land gain was vegetated land, 86% for the 1995 to 1999 period, and 66% for the 2004 to 2010 period. Vegetated land made up 56% to 83% of land lost, although this was on average only 9% of the total vegetated land. The period 1999 to 2004 was the exception where WLSD lost 8.0 km^2 of vegetated land, accounting for 16% of the total vegetated area in 1999. The vegetated land loss resulted in total net vegetated land loss of 4.9 km^2 at WLSD (Fig. 3B). On the other hand, a net vegetated land loss was not seen at ARSD throughout all four comparison periods. Net vegetated land gain accounted for 60% (1989–1995) to 91% (1999–2004) of the net land gain (Fig. 3A, B). The greatest open water to vegetated land gain for ARSD was 9.9 km^2 for a net vegetated land gain of 8.6 km^2 (1989–1995). The least amount of net vegetated land gain at ARSD occurred from 1999 to 2004 with 2.3 km^2 added to the subdelta (Fig. 3B). Vegetated land accounted for, on average, 62% of the land loss at ARSD, but this only amounted to 5.8% of the total vegetated surface.

4.4. Inter-periodic fluctuation of barren and vegetated land

Between the four periods, newly vegetated land was primarily sustained as vegetated land. At WLSD, 74% of newly vegetated land (i.e., water to vegetation) in 1995 was sustained as vegetated in 1999, and 67% of the newly vegetated land in 2004 was sustained as vegetated in 2010. The exception was the period 1999 to 2004 (Fig. 4). During this period, newly vegetated land from 1999 was converted to water at a slightly greater degree (47%) than being sustained as vegetated land (44%). The ARSD newly vegetated land was sustained as vegetated land for each period (71%, 1995 to 1999 and 94%, 2004 to 2010), although a slight decrease occurred from 1999 to 2004 (59%, Fig. 4). New barren land was for the most part converted to vegetated land during proceeding years except at WLSD. For 1999 to 2004 and for 2004 to 2010, WLSD new barren land was converted to water to a greater degree than vegetation (Fig. 4). Vegetated and barren land that was converted to water remained predominantly water in subsequent years (Fig. 5).

5. Discussion

The Atchafalaya River Delta complex is the only notable prograding delta feature along the Mississippi River Delta coastline in recent decades. For the past 21 years, our study found an average growth rate of the entire delta complex of 2.8 km^2 y^{-1}, which was slightly lower than two other recent estimates: 3.1 km^2 y^{-1} (1984–2004) by Xu (2010) and 3.2 km^2 y^{-1} (1985–2010) by Couvillion et al. (2011). The two subdeltas of the ARDC exhibited slightly different growth rates: 1.6 km^2 y^{-1} for ARSD and 1.2 km^2 y^{-1} for WLSD. Allen et al. (2012) had a similar estimated growth rate of 1.0 km^2 y^{-1} for WLSD (1983 to 2010), and Xu (2010) estimated growth rates for the period 1984 to 2004 of 1.1 km^2 y^{-1} (ARSD) and 2.0 km^2 y^{-1} (WLSD). Overall, differences in these growth rate estimates are small and can be attributed to different time frames and aerial coverage.

Delta growth fluctuation among the periods is of great interest. Delta growth had a clear decreasing trend from a high of 3.2 km^2 y^{-1} (WLSD) and 2.4 km^2 y^{-1} (ARSD) over the period 1989 to 1995 to a low of 0.6 km^2 y^{-1} (WLSD) and 1.6 km^2 y^{-1} (ARSD) over the period 2004 to 2010. Majersky et al. (1997) estimated similar rates for the earlier periods, 3.2 km^2 y^{-1} (ARSD) and 3.0 km^2 y^{-1} (WLSD); while Allen et al. (2012), looking at a

Table 3
Large flood events (>13,800 m^3 s^{-1} at Simmesport, LA) with dates of peak discharge.

Date	Period	Discharge peak (m^3 s^{-1})
6/11/1990	1989–1995	14,971
1/25/1991	1989–1995	16,244
5/18/1993	1989–1995	14,716
5/10/1994	1989–1995	13,895
6/17/1995	1989–1995	14,320
3/27/1997	1995–1999	18,027
2/15/1999	1995–1999	14,518
2/2/2005	2004–2010	14,914
4/24/2008	2004–2010	17,716
5/27/2009	2004–2010	15,650

Table 4
Land gain and loss for each period.

Land change (km^2)	1989–1995	1995–1999	1999–2004	2004–2010	1989–2010
Gain	37.3	24.1	14.5	20.0	62.0
Loss	3.7	9.5	16.6	7.1	3.1
Total change	33.6	14.6	−2.1	12.9	58.9
Annual change (km^2 y^{-1})	5.6	3.6	−0.4	2.1	2.8

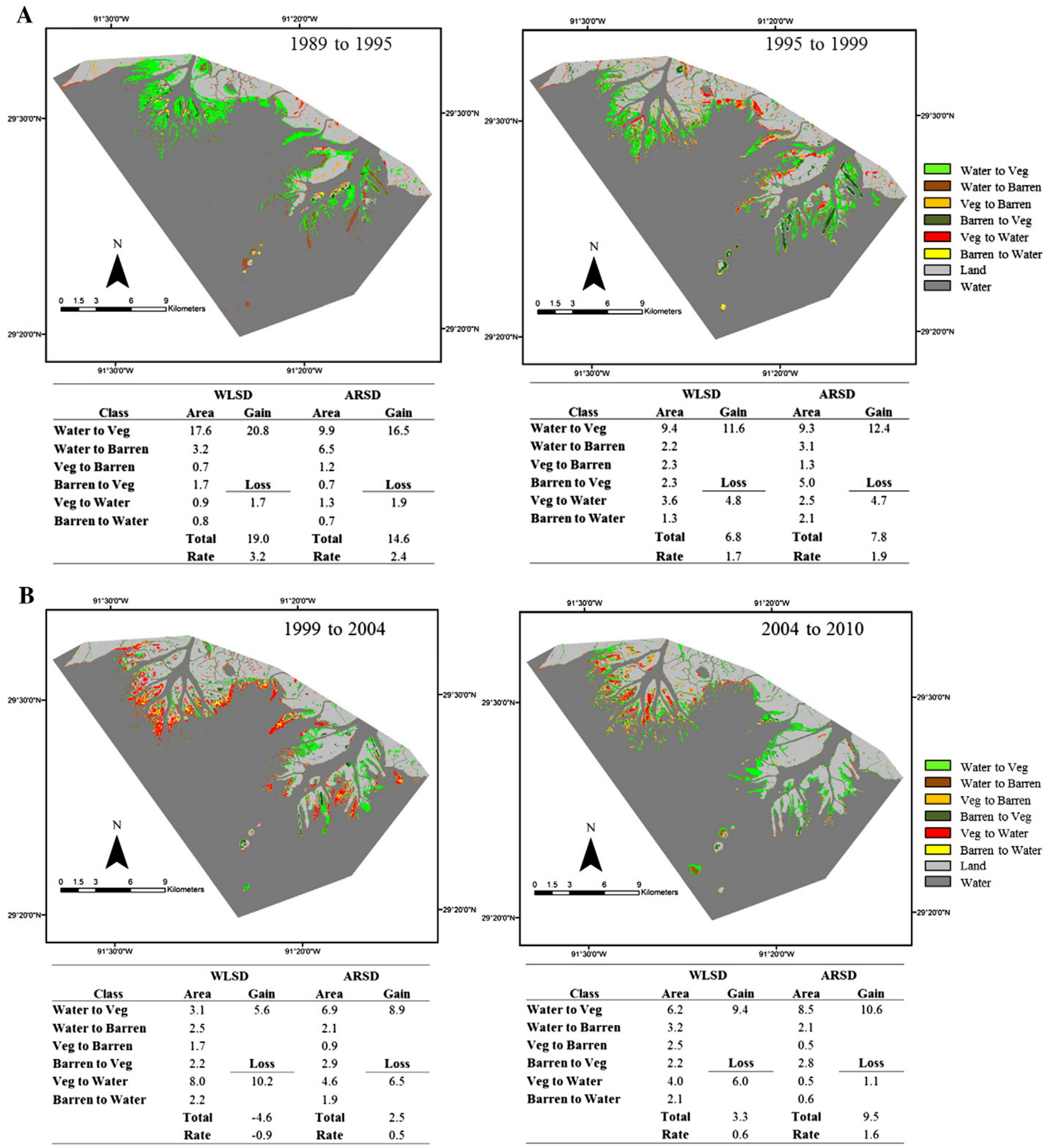

A — 1989 to 1995

	WLSD		ARSD	
Class	Area	Gain	Area	Gain
Water to Veg	17.6	20.8	9.9	16.5
Water to Barren	3.2		6.5	
Veg to Barren	0.7		1.2	
Barren to Veg	1.7	Loss	0.7	Loss
Veg to Water	0.9	1.7	1.3	1.9
Barren to Water	0.8		0.7	
	Total	19.0	Total	14.6
	Rate	3.2	Rate	2.4

1995 to 1999

	WLSD		ARSD	
Class	Area	Gain	Area	Gain
Water to Veg	9.4	11.6	9.3	12.4
Water to Barren	2.2		3.1	
Veg to Barren	2.3		1.3	
Barren to Veg	2.3	Loss	5.0	Loss
Veg to Water	3.6	4.8	2.5	4.7
Barren to Water	1.3		2.1	
	Total	6.8	Total	7.8
	Rate	1.7	Rate	1.9

B — 1999 to 2004

	WLSD		ARSD	
Class	Area	Gain	Area	Gain
Water to Veg	3.1	5.6	6.9	8.9
Water to Barren	2.5		2.1	
Veg to Barren	1.7		0.9	
Barren to Veg	2.2	Loss	2.9	Loss
Veg to Water	8.0	10.2	4.6	6.5
Barren to Water	2.2		1.9	
	Total	-4.6	Total	2.5
	Rate	-0.9	Rate	0.5

2004 to 2010

	WLSD		ARSD	
Class	Area	Gain	Area	Gain
Water to Veg	6.2	9.4	8.5	10.6
Water to Barren	3.2		2.1	
Veg to Barren	2.5		0.5	
Barren to Veg	2.2	Loss	2.8	Loss
Veg to Water	4.0	6.0	0.5	1.1
Barren to Water	2.1		0.6	
	Total	3.3	Total	9.5
	Rate	0.6	Rate	1.6

Fig. 3. Land change for the Wax Lake Outlet subdelta (WLSD) and Atchafalaya River subdelta (ARSD) for (A) 1989–1995 and 1995–1999 and (B) 1999–2004 and 2004–2010. All values are km^2 except for rate, km^2 y^{-1}. Gain is the sum of water to barren and water to vegetation and loss is the sum of barren to water and vegetation to water.

later period (2002–2010), found that WLSD had no net gain. From 1999 to 2004 the ARDC had a net loss of land, which was driven by large losses of land from the WLSD. During this period the growth rates dropped to -0.9 km^2 y^{-1} for WLSD and 0.5 km^2 y^{-1} for ARSD. The declined growth rate at ARSD depicts a part of a longer trend, where high early rates, estimated at 6.5 km^2 y^{-1} (1972 to 1976) (Rouse et al., 1978) and 5.8 km^2 y^{-1} (1976–1981) (Roberts et al., 1997) fell sharply following 1981 and has continued a slight decline to the latest period (Fig. 6). The WLSD had much slower development, but eventually eclipsed ARSD growth rate during the 1980s, but since the mid-1990s growth rate at WLSD has declined below ARSD growth rate, despite

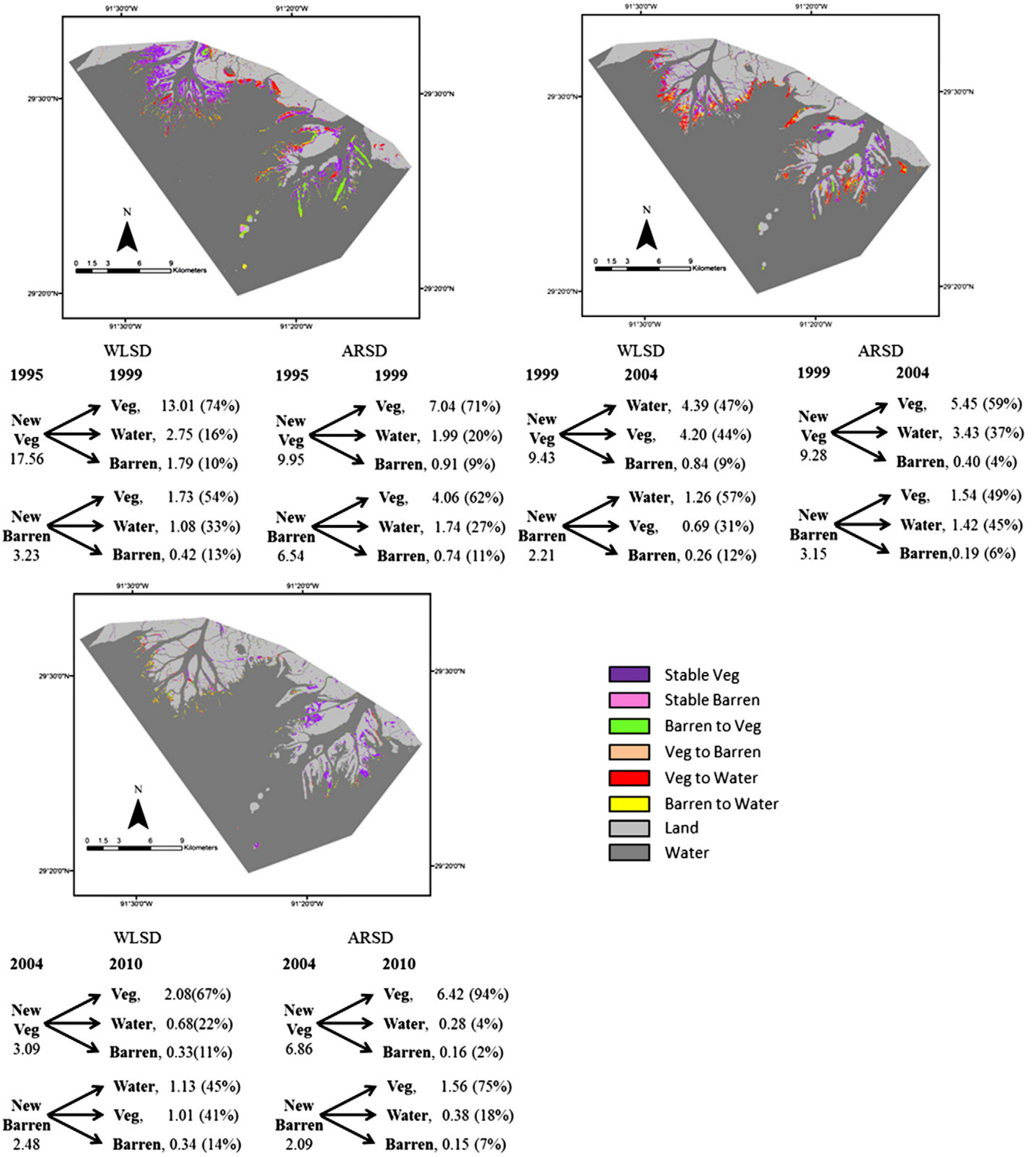

Fig. 4. Maps of how newly emergent land changed over time for each subdelta. *New Veg* is newly emergent vegetated land, and *New Barren* is newly emergent barren land. All values in km^2.

the increased portion of flow and sediment through WLO. The more stable growth rates at ARSD could be attributed to the many dredge spoil islands created from deposits of the Atchafalaya River bar channel. Further studies are needed to determine the management effect on land growth in the ARDC.

Among the four study periods, the 1999 to 2004 period was the only period without a large flood event (discharge > 13,800 m^3 s^{-1}) (Fig. 6). This period also had the highest recorded storm surge (3.75 m) caused by hurricane Lili in 2002 (SURGEDAT, 2012). During this period we found a net land loss at the ARDC (Table 4) solely because of the

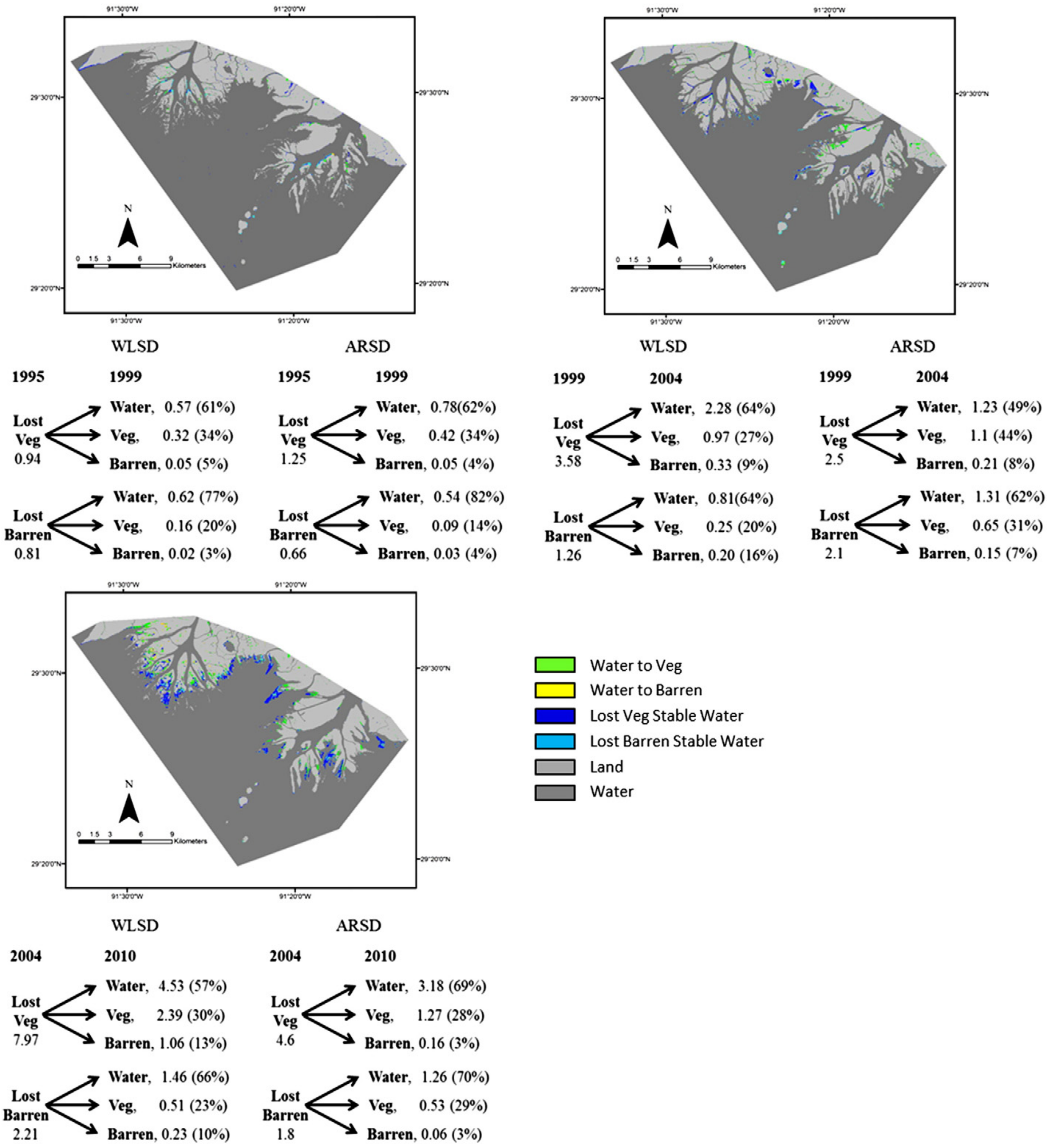

Fig. 5. Maps of how lost land changes over time for each subdelta. *Lost Veg* is vegetated land that was converted to water. *Lost Barren* is barren land that was converted to water. All values in km^2.

4.6 km^2 loss at WLSD (Fig. 3B). In other periods the transport capability of large floods was still able to maintain positive growth (Fig. 6). Rouse et al. (1978) indicated that the high growth rates observed during the initial stages of subaerial delta development (1972 to 1976) were fueled by two large floods over a three-year period. The 1975 flood was much larger than normal producing 11.4 km^2 of new land, whereas the smaller 1974 flood created only 2.6 km^2 (Rouse et al., 1978). It is well known that large flood events often provide the greatest sediment delivery, and periods with low flow can result in decreased delta growth, even in rivers with high SSC such as the Yellow River in China (Chu et al., 2005; Wang et

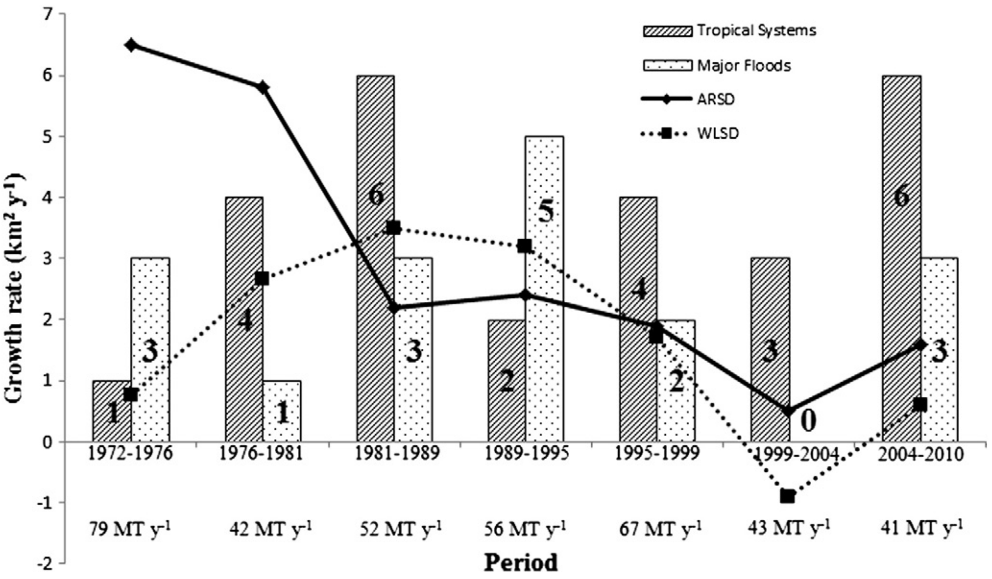

Fig. 6. Land growth rates for the Atchafalaya River subdelta (ARSD) and Wax Lake outlet subdelta (WLSD), number of tropical systems, and major floods (>13,800 m^3 s^{-1}) for seven periods starting from 1972 and ending in 2010. Period 1 = 1972–1976, period 2 = 1976–1981, period 3 = 1981–1989, period 4 = 1989–1995, period 5 = 1995–1999, period 6 = 1999–2004, and period 7 = 2004–2010. Average annual total suspended sediment yield is listed below the horizontal axis in megatonnes per year (MT y^{-1}). Growth rates for period 1 are from Rouse et al. (1978) (ARSD) and Roberts et al. (2003) (WLSD). Growth rates for period 2 and 3 are from Roberts et al. (2003). Tropical system counts are from Roth (2010) and average annual total suspended sediment yields prior to 1989 are from Xu (2010).

al., 2007). Nittrouer et al. (2008) identified that bedform transport rate of the lower Mississippi River had a positive exponential correlation with discharge, indicating the importance of large discharge events for delivering coarse load. This is evidenced in our study by the increase in suspended sand load with increasing discharge at ARMC and at WLO outlets (Fig. 7). The large quantity of coarse sediments provided by floods can be important for fueling delta growth by capping fine sediment deposits with a layer of coarse sediments that creates a substrate elevated enough for colonization of marsh species (van Heerden and Roberts, 1988). Our study suggests that river floods are a major contributing factor to the variation in deltaic growth rate of ARDC and that future growth of the ARDC will rely on a consistent frequency of large floods to counteract other stressors such as hurricanes, subsidence, and decreased SSC.

Tropical systems (hurricanes and tropical storms) have been documented causing variable affects to marshes, both physically destroying large areas (Barras, 2007; Howes et al., 2010) and supplying sediment (Rejmanek et al., 1988; Nyman et al., 1995; Turner et al., 2006). Over the four periods in this study, we found the most severe reduction in growth rate at the ARDC followed hurricane Lili in 2002. It was reported that the hurricane caused 7 km^2 of marsh loss ~21 km west of WLSD (Barras, 2003). Although there is no documentation of land loss at the ARDC, Lili and the two additional tropical storms (Table 1) that affected the area during the 1999–2004 period would have contributed to the negative growth rate. This is not a new phenomenon as observing growth rate estimates for previous periods would also seem to indicate that increases in tropical system frequency caused a reduction in growth rates (Fig. 6). The periods of 1999–2004 and 2004–2010 present an interesting contrast. The latter period had two category 3 hurricanes make land fall in 2005 (Table 1) causing 23 km^2 of land loss in the region around the ARDC (Barras, 2006), while the former only had one category 1 hurricane make land fall. Even with the land loss following the hurricanes during the 2004 to 2010 period, large flood events were able to counterbalance this loss to maintain a positive growth rate (Fig. 3B). This again indicates the dominant role of large flood events for maintaining growth at the ARDC.

Over the study period decreasing suspended sediment concentrations were observed at both subdeltas. The decreasing SSC observed over the period can be ascribed to decreasing SSC identified throughout the Mississippi River basin (Horowitz, 2010; Meade and Moody, 2010). The SSC decline directly affects total suspended sediment input to the ARDC. The Yellow River in China has also gone through a reduction in sediment discharge from 1000 MT y^{-1} to 150 MT y^{-1} (Wang et al., 2007), contributing to a gradual erosion phase at the Yellow River Delta since 1996 (Chu et al., 2005). The defining difference between the Yellow River and the Atchafalaya River is that flow and SSC of the Yellow River have declined greatly (Wang et al., 2007), whereas flow of the Atchafalaya River has stayed relatively constant over the past 21 years (Fig. 2). This has enabled the continuation of large flood pulses to occur in the Atchafalaya River. If total suspended sediment supply to the ARDC does not decrease further, growth rates of the delta complex should remain constant, as long as the flood pulse does not diminish.

Vegetation colonization of deltaic land occurred rapidly in ARDC, with 87% of the new subaerial land since 1989 vegetated. Between the four periods, vegetated land was not converted to water as readily as barren areas with, on average, only 7% of the vegetated land converted to water as compared to 32% of barren land. This may have been caused by greater sedimentation from vegetation influences and/or from the stabilizing effect of root density. In an early study on vegetation succession in newly created land, Johnson et al. (1985) found that biotic enhancement of sedimentation only occurred with *S. nigra* (black willow) on the highest elevation areas of the delta (e.g., levee), while the majority of delta sedimentation was controlled by physical processes, indicating different species effect. Even at lower elevations where sedimentation is controlled by physical processes, vegetation may still be important because McGinnis (1997) found that soil strength (ability to resist erosion) in a Louisiana coastal marsh was a function of live root density.

We found that newly vegetated areas maintained vegetation in subsequent periods at greater than 60% in the ARDC (Fig. 4). The only instance where newly vegetated land was converted to water at higher rates was during the 1999 to 2004 period (Fig. 4), where WLSD lost 4.4 km^2 of newly vegetated land. As discussed earlier, this period was characterized by a lack of large floods and three tropical system impacts. The combination of these factors could have

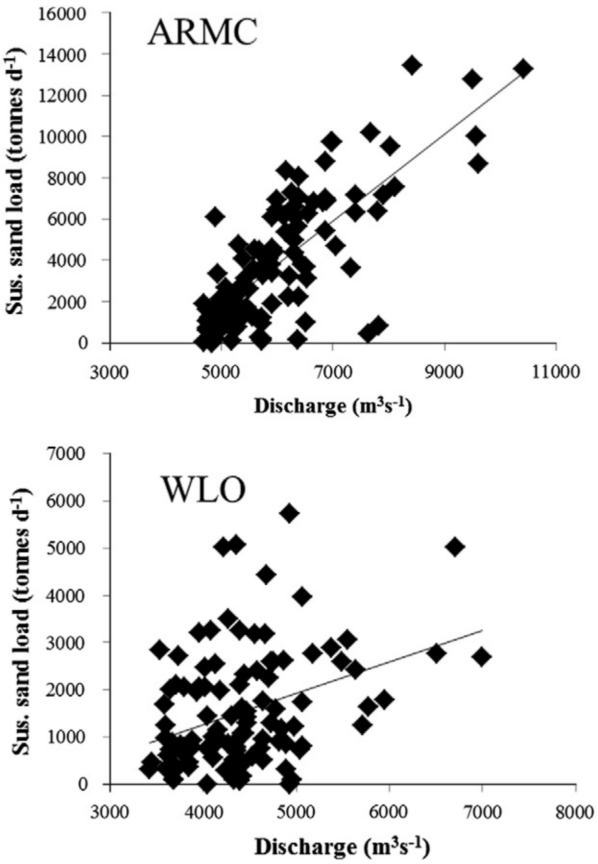

Fig. 7. Daily suspended sand load (grain size > 62.5 μm) versus water discharge above 25% discharge exceedance (1989–2010) for the Atchafalaya River Morgan City (ARMC) and Wax Lake outlet (WLO).

generated this loss by salt water stress causing vegetation mortality while lacking large flood events to provide large quantities of sediment. Hurricanes can cause extended periods of saltwater intrusion, which can kill freshwater marsh vegetation in addition to physically eroding away large areas of land (McKee and Mendelssohn, 1989; Flynn et al., 1995; Barras, 2007; Steyer et al., 2007). The land loss caused by tropical systems during the 1999 to 2004 period may not have been counterbalanced by enough sediment input in subsequent years from the lack of large flood pulses. In addition, the lower sediment input may not have been able to offset subsidence rates, which could exceed 6.0 mm y^{-1} from compaction of new delta surface (Shinkle and Dokka, 2004). This provides two important insights on vegetation stabilization of delta land. First, under reduced flow conditions vegetation alone may not be enough to maintain delta surface. This is supported by the findings of Neubauer (2008) that tidal freshwater marsh in active deltas in Louisiana was maintained through mineral additions. Second, that the stabilization displayed in other periods could have been land regeneration by large floods after high energy storm events followed by rapid vegetation colonization. Because of the lack of field surveys and a comparative design, our study cannot make a conclusive estimation as to the degree of vegetation stabilization in newly created land.

Two other factors may have affected our delta growth assessment: cold fronts and tidal variations. Cold front passage can cause water to flush out of the bay area and has been documented for being able to remove up to 10.6 MT of sediment annually from the Atchafalaya Bay (Walker and Hammack, 2000; Roberts et al., 2005). Unlike tropical systems and floods, cold fronts occur every year and the number that pass through Louisiana varies little between years, thus making their impacts relatively consistent and not a driving factor in the overall changes observed (Hardy and Henderson, 2003). Tides can also affect land estimates by affecting the amount of land surface visible. At the ARDC tide can cause the extent of land estimates to vary by as much as 30% (Allen et al., 2012), and this may have been the main cause for the small difference in delta growth rate estimates between this study's and others (Xu, 2010; Couvillion et al., 2011). During our four study periods, the difference in tides varied from 0.02 to 0.24 m. For the periods 1989 to 1995 and 1995 to 1999, each subsequent image had higher tide, which may have made the land estimates to be conservative. For the period 1999 to 2004, tide was the highest and may have exaggerated the net loss seen at the time. For the period 2004 to 2010, tide was the lowest for any image and thus could have caused a slight exaggeration of extent, adding to the gain seen during that period. The barren land class would have been affected by tide the most as these areas are most likely tidal flats so any variation in tide could have affected classification. Vegetated land was probably unaffected because the vegetation at lowest elevations (*S. platyphylla*, *N. lutea* and *S. latifolia*) grows taller (>0.8 m) than the tides observed, and thus variations in tides between images would not have caused these areas to be classified differently.

6. Conclusion

This study shows that the land growth of the Atchafalaya River Delta complex in the past two decades was dictated by large flood events, while severe tropical systems temporarily impacted delta size to a large degree. Large floods were able to transport substantial quantities of sediment needed to create rapid subaerial land formation, which was followed by vegetation colonization. When compared to barren land, vegetation succession provided stabilization. However, during the period with no large flood events the buffering effect of vegetation appeared to be limited against higher energy storm surges. The result implies that future growth and stabilization of the ARDC will mostly depend on sediment supply from the Atchafalaya River and storm weather conditions in the northern Gulf of Mexico. If sediment supply does decline in the future, delta growth will slow further and may also cause large flood events to be less effective at building land. Losses will likely be most apparent at WLSD that, unlike ARSD, does not have the additions of dredge spoil to create new land. With possible diversions of the Atchafalaya River water before reaching the subdeltas, future flood volumes might be reduced, slowing growth and possibly exacerbating erosion. Coastal Louisiana provides an interesting case study for other coastal regions around the world on how to manage sediment-starved deltas in the twenty-first century. With human and environmental factors both influencing delta evolution, creative and forward thinking river and sediment management will dictate the fate of coastal Louisiana and the millions of people that call it home.

Acknowledgments

The authors thank the United States Geological Survey and United States Army Corps of Engineers for making long-term data on river discharge and suspended sediment concentration available. Timothy Rosen received financial support from the Louisiana Sea Grant College Program during this study. The manuscript greatly benefited from the helpful comments and suggestions by two anonymous reviewers and from a very thorough editorial review by Dr. Richard A. Marston.

Appendix A

Table 1
Sediment rating curves used for estimation of total suspended sediment load ($t\ d^{-1}$) and subsequently summed to estimate annual total suspended sediment yield ($t\ y^{-1}$) for Atchafalaya River Morgan City (ARMC) and Wax Lake Outlet (WLO).

	ARMC			WLO		
Year	Sed. rating curves	r^2	% Diff[a]	Sed. rating curves	r^2	% Diff[a]
1989	$y = -0.4894x^2 + 10.317x - 40.489$	0.93	−0.58	$y = -0.5364x^2 + 9.9236x - 33.94$	0.79	1.40
1990	$y = 2.3654x - 8.3113$	0.92	−7.97	$y = 2.0552x - 5.3306$	0.92	−13.40
1991	$y = 1.7549x - 3.2172$	0.76	−0.31	$y = -0.5364x^2 + 9.9236x - 33.94$	0.79	−2.43
1992	$y = -0.289x^2 + 6.4414x - 22.148$	0.77	−1.39	$y = -0.5364x^2 + 9.9236x - 33.94$	0.79	−18.04
1993	$y = -0.3546x^2 + 7.7885x - 28.941$	0.92	1.01	$y = 1.6571x - 2.2451$	0.77	−1.18
1994	$y = -0.289x^2 + 6.4414x - 22.148$	0.77	5.22	$y = -0.5364x^2 + 9.9236x - 33.94$	0.79	3.35
1995	$y = 0.141x^2 - 0.9496x + 9.3784$	0.74	−2.12	$y = 1.4397x - 0.5$	0.80	1.90
1996	$y = 1.3711x - 0.1416$	0.73	−0.25	$y = 1.4397x - 0.5$	0.80	1.76
1997	$y = 0.141x^2 - 0.9496x + 9.3784$	0.74	−1.70	$y = 1.6571x - 2.2451$	0.77	0.94
1998	$y = 1.6558x - 2.1868$	0.71	0.52	$y = 1.7878x - 3.1357$	0.83	0.41
1999	$y = 1.6558x - 2.1868$	0.71	−9.70	$y = 1.7878x - 3.1357$	0.83	−3.99
2000	$y = 1.7549x - 3.2172$	0.76	8.73	$y = 1.6571x - 2.2451$	0.77	−0.32
2001	$y = -0.289x^2 + 6.4414x - 22.148$	0.77	−3.37	$y = 1.6571x - 2.2451$	0.77	−10.04
2002	$y = 1.8979x - 4.4989$	0.87	0.32	$y = -0.5364x^2 + 9.9236x - 33.94$	0.79	−1.23
2003	$y = 1.8979x - 4.4989$	0.87	13.92	$y = 1.9341x - 4.5948$	0.86	20.06
2004	$y = -0.1826x^2 + 4.5914x - 14.241$	0.92	3.46	$y = 1.479x - 1.0929$	0.90	−0.28
2005	$y = -0.289x^2 + 6.4414x - 22.148$	0.77	0.69	$y = 1.479x - 1.0929$	0.90	−1.04
2006	$y = 1.6849x - 2.7144$	0.91	No data	$y = -0.4022x^2 + 7.6626x - 24.747$	0.91	No data
2007	$y = 1.7549x - 3.2172$	0.76	−3.95	$y = 1.479x - 1.0929$	0.90	0.59
2008	$y = -0.289x^2 + 6.4414x - 22.148$	0.77	2.65	$y = 1.4665x - 1.0222$	0.68	−9.22
2009	$y = 0.0091x^2 + 1.5264x - 2.2121$	0.73	−3.45	$y = 1.4665x - 1.0222$	0.68	−0.21
2010	$y = 1.6758x - 2.8236$	0.73	−1.62	$y = 1.4665x - 1.0222$	0.68	8.36

[a] % Diff is the percent difference between estimated and measured total suspended sediment load.

References

Allen, Y.C., Couvillion, B.R., Barras, J.A., 2012. Using multitemporal remote sensing imagery and inundation measure to improve land change estimates in coastal wetlands. Estuaries and Coasts 35, 190–200.

Barras, J.A., 2003. Changes to Cote Blanche Hydrologic Restoration (TV-04) Area After Hurricane Lili. U.S. Geological Survey, National Wetlands Research Center, Map ID USGS NWRC 2003-11-112 (available online at http://www.nwrc.usgs.gov/special/200311-112).

Barras, J.A., 2006. Land area changes in coastal Louisiana after the 2005 hurricanes: A series of three maps. USGS Open File Report 2006–1274 (available online at http://pubs.usgs.gov/of/2006/1274/).

Barras, J.A., 2007. Land area changes in coastal Louisiana after Hurricanes Katrina and Rita. In: Farris, G.S., Smith, G.J., Crane, M.P., Demas, C.R., Robbins, L.L., Lavoie, D.L. (Eds.), Science and the Storms-The USFS Response to the Hurricanes of 2005. U.S. Geological Survey Circular 1306, pp. 98–113 (available online at http://pubs.usgs.gov/circ/1306/).

Chen, X., Zong, Y., 1998. Coastal erosion along the Changjiang deltaic shoreline, China: history and prospective. Estuarine, Coastal and Shelf Science 46 (5), 733–742.

Chu, Z.X., Sun, X.G., Zhai, S.K., Xu, K.H., 2005. Changing pattern of accretion/erosion of the modern Yellow River (Huanghe) subaerial delta, China: based on remote sensing images. Marine Geology 227, 13–30.

Coastal Protection and Restoration Authority of Louisiana (CPRA), 2012. Louisiana's Comprehensive Master Plan for a Sustainable Coast. Coastal Protection and Restoration Authority of Louisiana, Baton Rouge, LA.

Couvillion, B.R., Barras, J.A., Steyer, G.D., Sleavin, W., Fischer, M., Beck, H., Trahan, N., Griffin, B., Heckman, D., 2011. Land Area Change in Coastal Louisiana from 1932 to 2010. U.S. Geological Survey Scientific Investigations Map 3164, scale 1:265,000, pp. 1–12. pamphlet.

Day, J.W., Pont, D., Hensel, P.F., Ibanez, C., 1995. Impacts of sea-level rise on deltas in the Gulf of Mexico and the Mediterranean — the importance of pulsing events to sustainability. Estuaries 18 (4), 636–647.

Duan, N., 1983. Smearing estimate: a nonparametric retransformation method. Journal of the American Statistical Association 78 (383), 605–610.

Fisk, H.N., 1952. Geological Investigation of the Atchafalaya Basin and the Problem of Mississippi River Diversion. Mississippi River Commission, Vicksburg, MS (145 pp.).

Flynn, K.M., McKee, K.L., Mendelssohn, I.A., 1995. Recovery of freshwater marsh vegetation after a saltwater intrusion event. Oecologia 103, 63–72.

Ford, M., Nyman, J.A., 2011. Preface: an overview of the Atchafalaya River. Hydrobiologia 658, 1–5.

Galloway, W.E., 1975. Process framework for describing the morphologic and stratigraphic evolution of deltaic depositional systems. In: Broussard, M.L. (Ed.), Deltas, Models for Exploration. Houston Geological Society, pp. 87–98.

Glysson, G.D., 1987. Sediment-transport curves. USGS Open File Report 87-218, Reston, VA.

Gornitz, V., 1995. Sea-level rise — a review of recent past and near-future trends. Earth Surface Processes and Landforms 20 (1), 7–20.

Guntenspergen, G.R., Cahoon, D.R., Grace, J., Steyer, G.D., Fournet, S., Townson, M.A., Foote, A.L., 1995. Disturbance and recovery of the Louisiana coastal marsh landscape from the impacts of Hurricane Andrew. In: Stone, G.W., Finkl, C.W. (Eds.), Impacts of Hurricane Andrew on the Coastal Zone of Florida and Louisiana: 22–26 August 1992: Journal of Coastal Research, Special Issue No. 21, pp. 324–339.

Hardy, J.W., Henderson, K.G., 2003. Cold front variability in the southern United States and the influence of atmospheric teleconnection patterns. Physical Geography 24 (2), 120–137.

Heimann, D.C., Sprague, L.A., Blevins, D.W., 2011. Trends in Suspend-Sediment Loads and Concentrations in the Mississippi River Basin, 1950–2009. U.S. Geological Survey Scientific Investigations Report 2011-5200, pp. 1–33.

Helsel, D.R., Hirsch, R.M., 2002. Statistical methods in water resources. Techniques of Water-Resources Investigations of the USGS, Reston, VA, pp. 221–263 (available online at http://pubs.usgs.gov/twri/twri4a3/pdf/twri4a3-new.pdf).

Helsel, D.R., Mueller, D.K., Slack, J.R., 2006. Computer Program for the Kendall Family of Trend Tests. USGS Scientific Investigations Report, 2005–5275, Reston, VA, pp. 1–4.

Horowitz, A.J., 2003. An evaluation of sediment rating curves for estimating suspended sediment concentrations for subsequent flux calculations. Hydrological Processes 17, 3387–3409.

Horowitz, A.J., 2010. A quarter century of declining suspended sediment fluxes in the Mississippi River and the effect of the 1993 flood. Hydrological Processes 24, 13–34.

Howes, N.C., FitzGerald, D.M., Hughes, Z.J., Georgiou, I.Y., Kulp, M.A., Miner, M.D., Smith, J.M., Barras, J.A., 2010. Hurricane-induced failure of low salinity wetlands. PNAS 107 (32), 14014–14019.

Johnson, W.B., Sasser, C.E., Gosselink, J.G., 1985. Succession of vegetation in an evolving river delta, Atchafalaya Bay, Louisiana. Journal of Ecology 73 (3), 973–986.

Kesel, R.H., 2003. Human modifications to the sediment regime of the lower Mississippi River flood plain. Geomorphology 56, 325–334.

Majersky, S., Roberts, H.H., Cunningham, R., Kemp, G.P., John, C.J., 1997. Facies development in the Wax Lake Outlet delta: present and future trends. Basin Research Institute Bulletin 7, 50–66.

McGinnis II, T.E., 1997. Factors of Soil Strength and Shoreline Movement in a Louisiana Coastal Marsh. (M.S. thesis) University of Southwestern Louisiana, Lafayette, LA, USA.

McKee, K.L., Mendelssohn, I.A., 1989. Response of a freshwater marsh plant community to increased salinity and increased water level. Aquatic Botany 34 (4), 301–316.

Meade, R.H., Moody, J.A., 2010. Causes for the decline of suspended-sediment discharge in the Mississippi River system, 1940–2007. Hydrological Processes 24 (1), 35–49.

Miller, C.R., 1951. Analysis of Flow-Duration Sediment-Rating-Curve Method of Computing Sediment Yield. U.S Dept. of Interior, Bur. of Reclamation, Washington, DC (55 pp.).

Morton, R.A., Bernier, J.C., 2010. Recent subsidence-rate reduction in the Mississippi Delta and their geological implications. Journal of Coastal Research 26 (3), 555–561.

Mossa, J., Roberts, H.H., 1990. Synergism of riverine and winter storm-related sediment transport processes in Louisiana's coastal wetlands. Transactions Gulf Coast Association of Geological Societies 40, 635–642.

Neill, C.F., Allison, M.A., 2005. Subaqueous deltaic formation on the Atchafalaya Shelf, Louisiana. Marine Geology 214, 411–430.

Neubauer, S.C., 2008. Contributions of mineral and organic components to tidal and freshwater marsh accretion. Estuarine, Coastal and Shelf Science 78, 78–88.

Nittrouer, J.A., Allison, M.A., Campanella, R., 2008. Bedform transport rates for the lowermost Mississippi River. Journal of Geophysical Research 113, 1–16.

Nyman, J.A., Crozier, C.R., DeLaune, R.D., 1995. Roles and patterns of hurricane sedimentation in an estuarine marsh landscape. Estuarine, Coastal and Shelf Science 40 (6), 665–679.

Orton, G.J., Reading, H.G., 1993. Variability of deltaic processes in terms of sediment supply, with particular emphasis on grain size. Sedimentology 40, 475–512.

Rejmanek, M., Sasser, C.E., Peterson, G.W., 1988. Hurricane-induced sediment deposition in a gulf coast marsh. Estuarine, Coastal and Shelf Science 27 (2), 217–222.

Roberts, H.H., Adams, R.D., Cunningham, R.H.W., 1980. Evolution of sand-dominant subaerial phase, Atchafalaya Delta, Louisiana. American Association of Petroleum Geologists Bulletin 64 (2), 264–279.

Roberts, H.H., Walker, N.D., Cunningham, R., Kemp, G.P., Majersky, S., 1997. Evolution of sedimentary architecture and surface morphology: Atchafalaya and Wax Lake Deltas, Louisiana (1973–1994). Gulf Coast Association of Geological Societies Transactions 47, 477–484.

Roberts, H.H., Coleman, J.M., Bentley, S.J., Walker, N., 2003. An embryonic major delta lobe: a new generation of delta studies in the Atchafalaya-Wax Lake Delta System. Gulf Coast Association of Geological Societies Transactions 53, 690–703.

Roberts, H.H., Walker, N.D., Sheremet, A., Stone, G.W., 2005. Effects of cold fronts on bayhead delta development: Atchafalaya Bay, Louisiana, USA. In: FitzGerald, D.M., Knight, J. (Eds.), Coastal Systems and Continental Margins, High Resolution Morphodynamics and Sedimentary Evolution of Estuaries 8. Springer, Dordrecht, Netherlands, pp. 269–298.

Roth, D., 2010. Louisiana Hurricane History. National Weather Service (available online at: http://www.hpc.ncep.noaa.gov/research/lahur.pdf).

Rouse, L.J., Roberts, H.H., Cunningham, R.H.W., 1978. Satellite observation of the subaerial growth of the Atchafalaya Delta, Louisiana. Geology 6, 405–408.

Shinkle, K.D., Dokka, R.K., 2004. Rates of vertical displacement at benchmarks in the Lower Mississippi Valley and the Northern Gulf Coast. NOAA Technical Report NOS/NGS 50, Washington, DC (147 pp.).

Shlemon, R.J., 1975. Subaqueous delta formation-Atchafalaya Bay, Louisiana. In: Broussard, M.L. (Ed.), Deltas: Models of Exploration. Houston Geological Society, Houston, TX, pp. 209–221.

Smith, S.E., Abdel-Kader, A., 1988. Coastal erosion along the Egyptian delta. Journal of Coastal Research 4 (2), 245–255.

Steyer, G.D., Perez, B.C., Piazza, S., Suir, G., 2007. Potential consequences of saltwater intrusion associated with hurricanes Katrina and Rita. In: Farris, G.S., Smith, G.J., Crane, M.P., Demas, C.R., Robbins, L.L., Lavoie, D.L. (Eds.), Science and the Storms — The USFS Response to the Hurricanes of 2005: U.S. Geological Survey Circular 1306, Reston, VA, pp. 98–113 (available online at http://pubs.usgs.gov/circ/1306/pdf/c1306_ch6_c.pdf).

SURGEDAT, 2012. Comprehensive storm surge database. http://surge.srcc.lsu.edu/ (last accessed on August 2, 2012).

Syvitski, J.P.M., Kettner, A.J., Overeem, I., Hutton, E.W.H., Hannon, M.T., Brakenridge, G.R., Day, J., Vorosmarty, C., Saito, Y., Giosan, L., Nicholls, R.J., 2009. Sinking deltas due to human activities. Nature Geoscience. http://dx.doi.org/10.1038/NGEO629.

Törnqvist, T.E., Kidder, T.R., Autin, W.J., Van der Borg, K., de Jong, A.F.M., Klerks, C.J.W., Snijiders, E.M.A., Storms, J.E.A., van Dam, R.L., Wiemann, M.C., 1996. A revised chronology for Mississippi River subdeltas. Science 273, 1693–1696.

Törnqvist, T.E., Wallace, D.J., Storms, J.E.A., Wallinga, J., Van Dam, R.L., Blaauw, M., Derksen, M.S., Klerks, C.J.W., Meijneken, C., Snijders, E.M.A., 2008. Mississippi Delta subsidence primarily caused by compaction of Holocene strata. Nature Geoscience 1, 173–176.

Turner, R.E., Baustian, J.J., Swenson, E.M., Spicer, J.S., 2006. Wetland sedimentation from hurricanes Katrina and Rita. Science 314 (5798), 449–452.

Tye, R.S., Coleman, J.M., 1989. Depositional processes and stratigraphy of fluvially dominated lacustrine deltas: Mississippi Delta Plain. Journal of Sedimentary Petrology 59 (6), 973–996.

van Heerden, I.L., Roberts, H.H., 1980. The Atchafalaya Delta — Louisiana's new prograding coast. Transactions-Gulf Coast Association of Geological Societies 30, 497–505.

van Heerden, I.L., Roberts, H.H., 1988. Facies development of Atchafalaya Delta, Louisiana: a modern bayhead delta. American Association of Petroleum Geologists Bulletin 72 (4), 439–453.

Walker, N.D., 2001. Tropical storm and hurricane wind effects on water level, salinity, and sediment transport in the river-influenced Atchafalaya–Vermilion Bay system, Louisiana, USA. Estuaries 24 (4), 498–508.

Walker, N.D., Hammack, A.B., 2000. Impacts of winter storms on circulation and sediment transport: Atchafalaya–Vermilion Bay region, Louisiana. Journal of Coastal Research 16 (4), 996–1010.

Walling, D.E., Fang, D., 2003. Recent trends in the suspended sediment loads of the world rivers. Global and Planetary Change 39 (1–2), 111–126.

Wang, H., Yang, Z., Saito, Y., Liu, J.P., Sun, X., Wang, Y., 2007. Stepwise decreases of the Huanghe (Yellow River) sediment load (1950–2005): Impacts of climate change and human activities. Global and Planetary Change 57, 331–354.

Xu, Y.J., 2010. Long-term Sediment Transport and Delivery of the Largest Distributary of the Mississippi River, the Atchafalaya, USA. In: Banasik, K., Horowitz, A., Owens, P.N., Stone, M., Walling, D.E. (Eds.), Sediment Dynamics for a Changing Future, 337. IAHS Publication, Wallingford, UK, pp. 282–290.

Xu, Y.J., BryantMason, A., 2011. Determining the Nitrate Contribution of the Red River to the Atchafalaya River in the Northern Gulf of Mexico under Changing Climate. In: Peters, J. (Ed.), Water Quality: Current Trends and Expected Climate Change Impacts, 348. IAHS Publication, Wallingford, UK, pp. 95–100.

Xu, Y.J., Wang, F., 2013. Transport and delivery of suspended sediment to Atchafalaya Bay of the northern Gulf of Mexico. Journal of Hydrology (in review).

Yuill, B., Lavoie, D., Reed, D.J., 2009. Understanding subsidence processes in coastal Louisiana. Journal of Coastal Research 54, 23–36.